Structure and Dynamics of Force Clusters and Networks in Shear Thickening Suspensions

Mohammad Nabizadeh,[1] Abhinendra Singh,[2,†] and Safa Jamali[1,*]
[1]Department of Mechanical and Industrial Engineering, Northeastern University, Boston, Massachusetts 02115, USA
[2]James Franck Institute and Pritzker School of Molecular Engineering, The University of Chicago, Chicago, Illinois 60637, USA

(Received 18 April 2022; accepted 13 July 2022; published 2 August 2022)

Dense suspensions can exhibit shear thickening in response to large deformation. A consensus has emerged over the past few years on the formation of force networks, that span the entire system size, that lead to increased resistance to motion. Nonetheless, the characteristics of these networks are to a large extent poorly understood. Here, force networks formed in continuous and discontinuous shear thickening dense suspensions (CST and DST, respectively) are studied. We first show the evolution of the network formation and its topological heterogeneities as the applied stress increases. Subsequently, we identify force communities and coarse grain the suspension into a cluster network, and show that cluster-level dynamics are responsible for stark differences between the CST and DST behavior. Our results suggest that the force clusters formed in the DST regime are considerably more constrained in their motion, while CST clusters are loosely connected to their surrounding clusters.

DOI: 10.1103/PhysRevLett.129.068001

Dense suspensions of particles are ubiquitous in many industrial, natural, and biological problems [1,2]. These dense suspensions can exhibit a rich set of rheological signatures that include yielding, shear thinning or thickening, and shear jamming [1,3–5]. These non-Newtonian rheological features often find their underpinnings in the interfacial and surface properties of the individual particles and the way they interact with one another [5–14]. The increase in the suspension viscosity at a given volume fraction ϕ can be smooth or abrupt, termed as continuous shear thickening (CST) and discontinuous shear thickening (DST), respectively. In particular, DST has recently been related to the stress-activated transition from an unconstrained lubricated state to a constrained state where relative motion of particles in the tangential pairwise direction is significantly hindered beyond an "onset stress" [5–7,15]. This constrain on the motion of particles can be caused by frictional contacts [16,17] or lubrication forces at the particle roughness level [9]. Nonetheless, this constraint-based picture of the suspension rheology through mean-field approaches has been successful in describing both simulation and experimental data [15,18–20]. What is clear is that these particle-level interactions in turn result in large scale force and contact networks that resist large deformations and hence increase the viscosity of the suspension [21]. However, how this force or contact network emerges and its characteristics are unexplored. An important fundamental question is the difference in the force network when the suspension undergoes continuous or discontinuous shear thickening. Some recent works have shown that there exists a connection between the underlying network structure and the rheology of shear thickening suspensions rheology [22–24]. In particular, the work of Sedes *et al.* [24] showed that a K-core analysis can be used for clustering particles in contact within a percolated network. On the other hand, several well-established methodologies exist for clustering different components of a complex network. Network science studies the network of interacting constituents through their patterns of connection [25,26]. This provides us with the opportunity of applying network science techniques on the force networks in dense suspensions, where characteristics of the particle-level dynamics cannot provide enough explanation to the emergence of shear thickening [17]. Network science techniques have been employed in a wide variety of scientific studies from the world wide web, to biological systems, neuroscience, and structured materials [27–31]. In many cases, complex behavior of the interaction networks originates not only from the interactions between individual parts of the network, but also formation of communities of individuals that interact with one another, and unveil hidden characteristics of the network [32,33]. Community detection algorithms are applicable in the context of dense suspensions because the rate-dependent viscosity of such materials are shown to originate from the resistance of clusters of particles against fluid flow [34]. Application of network science tools in the study of granular matter is demonstrated by Papadopoulos *et al.* [31] where community structure detection algorithms have been shown to successfully identify mesoscale structures from the network of frictional contacts. In this Letter, we employ a series of network science techniques to explore formation and evolution of frictional contact networks using simulations of dense suspensions. First, we investigate the force network as a whole as the applied stress is increased and with respect to the shear-thickening behavior. Then we adapt a Gaussian mixture model (GMM) algorithm to detect force clusters and use these communities to distinguish between CST and DST suspensions.

Although real-world shear thickening (ST) systems are 3D, the main rheological features of 2D suspensions are found to be very similar to these real systems [23]. As the system evolves in all three dimensions, additional contacts are made between particles. Nonetheless, dynamics of force contacts and clusters can be more easily conceptualized and studied with respect to their constraints in a lower dimensional flow. As such, and for the sake of clarity and simplicity here we use 2D simulation of dense suspensions, performed in a series of stress-controlled simple shear flows for two area fractions of particles, $\phi_A = 0.72$, 0.78 with $N = 2000$ bidisperse (radii a and $1.4a$) spherical rigid non-Brownian particles. Here, the equation of motion is the force balance between hydrodynamics ($\mathbf{F}_H$) and contact ($\mathbf{F}_C$) forces on each particle. Rate dependence is introduced by employing a critical load model where the normal force must exceed force threshold F_0 to activate friction between particles [16,17]. Further details about the simulation scheme are available in Supplemental Material [35]. For the lower area fraction, $\phi_A = 0.72$, the shear viscosity increases gradually with increase of the applied shear stress indicating a CST behavior. On the other hand, at higher area fraction of $\phi_A = 0.78$ there is a discontinuous jump in viscosity, and a S-shaped flow curve indicative of the DST behavior [18,19]. A series of computational and experimental studies [8–10,16,17,34,43–46] have shown the emergence of a percolated network of contacts between the particles in the shear thickened state (STS). Here, the focus is on characterization of these networks formed by the interparticle frictional contacts. We convert the physical system of particles and interparticle force contacts to a network, where particles and interparticle forces and contacts are represented by nodes and edges, respectively. Networks of stress-induced frictional contacts before ST, at the onset of ST, and deep into the shear-thickened state, for both CST ($\phi_A = 0.72$), and DST ($\phi_A = 0.78$) are shown in the snapshots of Fig. 1, where the frictional bonds between contacting particles are colored in red. Clearly, as the shear stress increases, we go from a frictionless, low viscosity regime, to emergence of frictional contacts leading to shear thickening, and eventually to a high viscosity rate-independent contact-dominated regime. Hence, the evolution of those networks seems be providing the constraints leading to ST. From a visual inspection, the force networks at the higher area fraction appear to be denser both at the onset of ST, and in the shear-thickened state.

We employ various network measures to quantify the density of contacts and also their patterns of connections. Figure 2(a) shows the average number of contacts per particle versus shear stress. In both CST and DST, increasing the applied stress increases the number of frictional contacts at the onset of ST, although the rate by which contacts are added is significantly less at higher stresses, and the average coordination number becomes nearly constant in the shear-thickened state. This is consistent

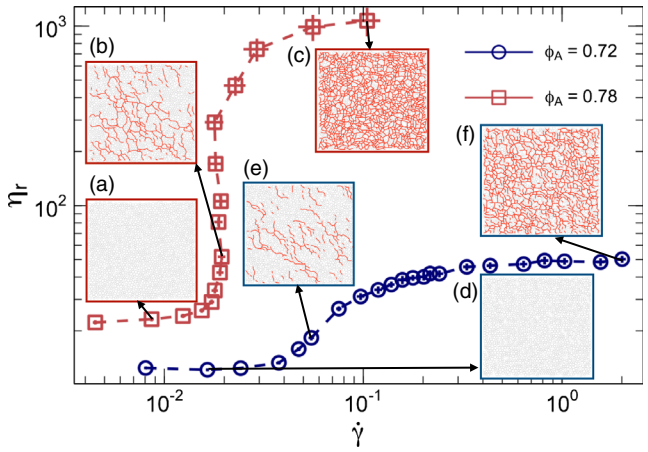

FIG. 1. (a) Relative viscosity versus shear rate for two different area fractions, showing CST and DST. Snapshots of the network of frictional contacts for $\phi_A = 0.72$ (a), (b), (c) and $\phi_A = 0.78$ (d), (e), (f) at applied stresses of 0.1 (a), (d), 1 (b), (e), and 100 (c), (f).

with the measurements of 3D systems in [24]. On average, and deep into the STS, each particle in the DST regime has ~0.8 compared to the CST system, $\langle Z_{\mathrm{DST}}^{\mathrm{STS}} \rangle = \langle Z_{\mathrm{CST}}^{\mathrm{STS}} \rangle + 0.8$. Although particle-level contacts provide some insight into the state of suspension, the force chains will need to become significant compared to the system size for the suspension viscosity to rise. As clearly visible in Figs. 1(c) and 1(f) these contacts can be disconnected and interspersed within the suspension, but eventually percolate to span the entire system. As such, the essential load-bearing component to the viscosity is the largest connected component (LCC) of particles. The largest connected component of the network, normalized by the total number of particles within the system is shown in Fig. 2(b). LCC of both CST and DST networks grow with stress, with 80%–90% of the particles belonging to one percolated network at the largest stresses applied. Nonetheless, there are no significant differences in the evolution or the size of the LCC in CST compared to the DST networks. Sedes *et al.* [24] showed that the network susceptibility shows a divergence at the percolation point, and a network homology study [23] on shear thickening suspension suggested that long-lived contact loops emerge at the onset of shear thickening as well. The longest path connecting any two components within a system can be used as an alternative measure of the network heterogeneity. This is commonly referred to as the diameter of the network [27]. For a percolated network, generally a shorter network diameter would result in enhanced connectivity of the system. As such, in addition to a significant LCC, diameter can be used as a measure of network's ability to transmit stresses more effectively. This argument is valid from a physical perspective as well: consider a cluster of particles that are closely connected to one another in a dense packing, with relatively short paths to travel from one node to another.

In this scenario, restriction of a particle highly affects the motion of the other particles. Alternatively, particles connected in a chainlike packing require longer walks to go from one node to another. The latter structure geometrically poses fewer restrictions on the motion of other particles, when any of the cluster's components are constrained. Figure 2(c) shows the diameter of force networks for the two systems studied normalized by the size of the calculation box, indicating that for both CST and DST, the network diameter grows before the onset of shear thickening and shortly after percolation. Note that the largest diameter of the DST network measured grows larger than the calculation box, suggesting an elongated chainlike network of contacts at the early stages of shear thickening. However, as more contacts form and loops emerge, additional edges will provide shorter node to node paths for the same particles that were already connected through longer path(s). While both of the networks show similar trends, this is more clear and significant for the DST suspension. Wang *et al.* [10] showed that stresses in shear-thickening suspensions are heterogeneous at the onset and early stages of shear thickening, and become increasingly homogeneous in the STS. This is consistent with the diameter of the network measured in Fig. 2(c).

While characteristics of the force networks in CST and DST show differences in the density of contacts and the rate by which they grow during ST, these differences cannot describe stark differences in the stress response of these two systems. It is plausible to assume formation of particle clusters that are the primary units for resistance to motion [2,47,48]. For attractive colloidal gels, these particle clusters have been shown to be responsible for the emergence of rigidity [49]. Therefore, it is appropriate to identify force clusters within the percolated network of ST suspensions. This in network analysis is commonly referred to as "community" detection, which involves identification of nodes within a larger network that share similar modularity. There are many different methods of community detection in general [50], and different methods that can be applied to particulate and granular systems are reviewed in [51]. In this Letter, we employ a Gaussian mixture model (GMM) algorithm in order to robustly identify the force and contact clusters. For details of the GMM algorithm and how it identifies the number and constituents of particle clusters refer to Supplemental Material [35]. Snapshots of the particle clusters are shown for both CST and DST systems in Figs. 3(a) and 3(b), respectively, where particles that belong to one cluster are colored similarly for visual purposes. The CST clusters are seemingly relatively more elongated compared to the DST clusters. The GMM recovers a growing number of clusters as the stress is increased for both systems, with a quasisteady value in the STS [Fig. 3(c)]. Having the clusters clearly identified, we further characterize the clusters in each system and under different stresses applied. The number of particles per cluster is measured as the cluster mass, M_{cluster}, and plotted for different stresses in Fig. 3(d). For the CST system, the cluster sizes gradually grow as the stress is increased (although viscosity remains constant); however, for the DST system the cluster size immediately finds a well-defined and steady distribution in the STS whose mean value is significantly larger than the CST clusters. The diameter of the cluster D_{cluster} defined as the diameter of a single circle to encompass all nodes within a cluster, however, shows a rather similar and steady distribution for both CST and DST [Fig. 3(e)]. These two measures together enable calculation of an internal area fraction of clusters. We find that DST clusters are more densely packed and locally have higher area fractions [Fig. 3(f)]. Note that these are elongated clusters whose individual area fractions are significantly less than the overall area fraction of the system, and thus the total area fraction of the clusters sum up to more than $\phi^{\text{total}}_{\text{clusters}} > 3$, as shown in Fig. 3(g). These locally more packed DST clusters also can be quantified through higher fractal dimensions [Fig. 3(h)], where fractal dimension is defined as $\log(M_{\text{cluster}})/\log(D_{\text{cluster}})$.

Regardless of how dense clusters are, or how many clusters exist within a network, it is their connectivity that ultimately controls the rheological response of the entire

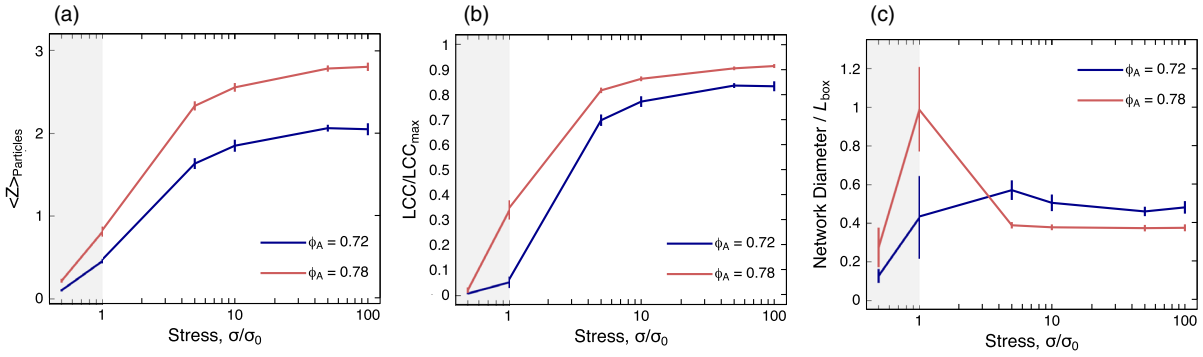

FIG. 2. (a) Average number of contacts per particle, (b) normalized largest connected component, and (c) normalized network diameter against imposed shear stress.

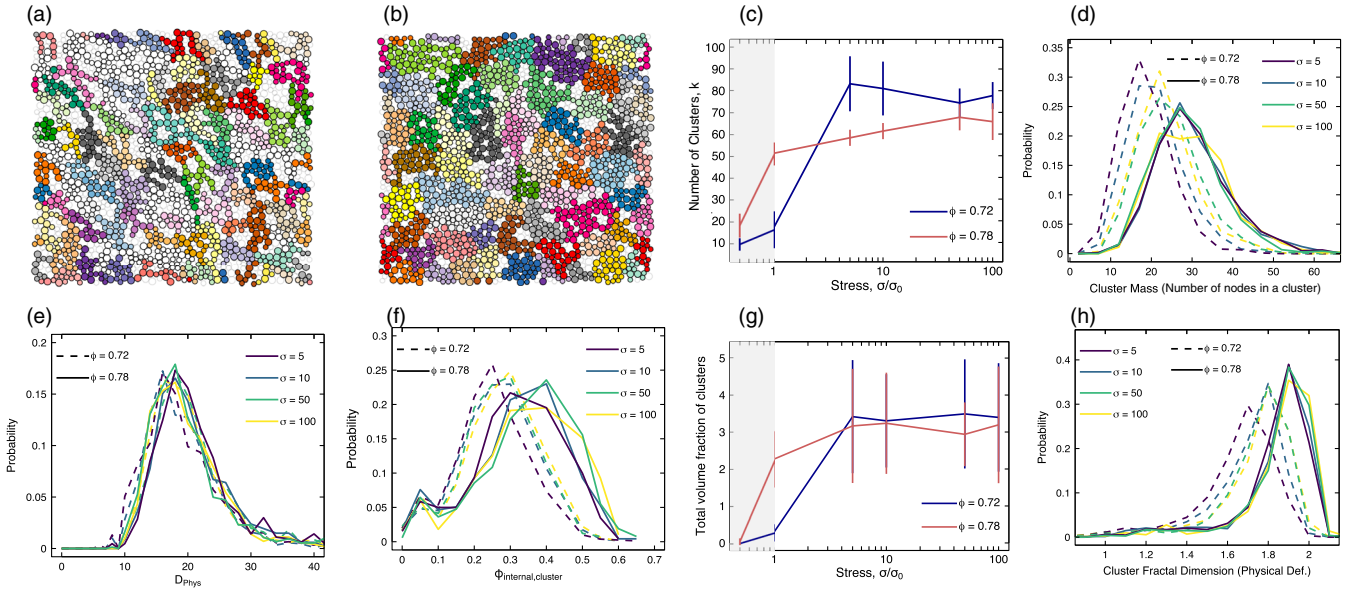

FIG. 3. Snapshots of the system after clustering for suspensions showing (a) CST, and (b) DST behavior (particles of the same cluster are colored similarly). (c) Number of clusters versus shear stress, (d) distribution of cluster mass, (e) distribution of cluster diameters, (f) internal local area fraction of clusters, (g) total area fraction of all clusters, and (h) the internal fractal dimension of clusters for two different area fractions in the CST and DST regime.

suspension. Here, we consider clusters i and j to be in contact, if there exists at least one particle-level contact connecting their constituents. For instance, in Figs. 4(a) and 4(b), individual black circles represent the clusters' center of mass, and an edge is added between two clusters if there exists at least one particle-particle contact between two clusters. This provides a *coarse-grained* view of the particulate network. Although CST suspensions yield more number of clusters, the total number of contacting neighbors, $\langle Z_{\text{clusters}} \rangle$, for the DST is clearly larger as plotted in Fig. 4(c). This suggests that clusters in DST are significantly more interconnected compared to the CST clusters.

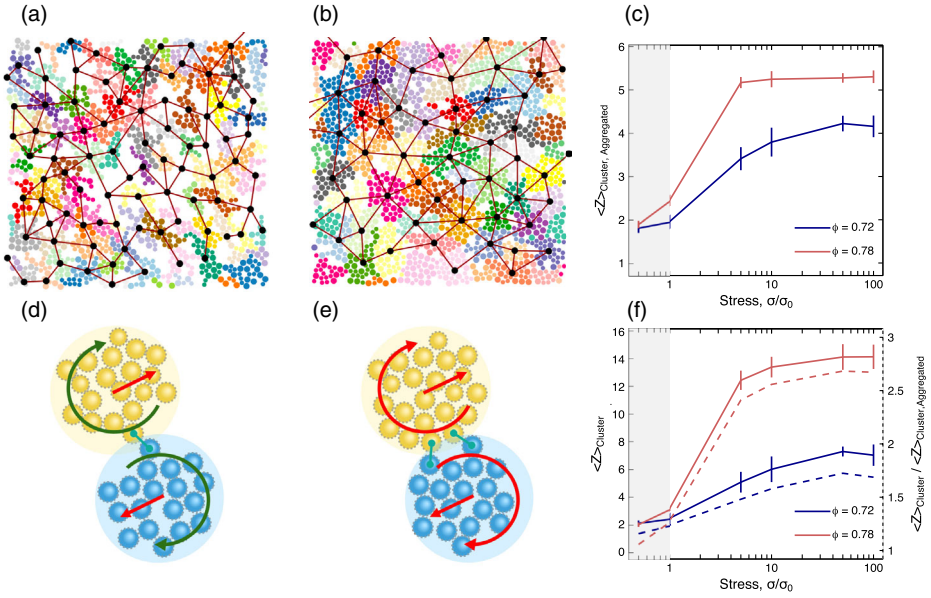

FIG. 4. Snapshots of clusters and their contacts for (a) CST and (b) DST suspensions. (c) The average number of neighbors per cluster versus shear stress. The schematic depiction of constrained cluster motion based on (d) single or (e) multiple particle-level contacts connecting two neighboring clusters. Straight arrows show the relative sliding motion, and the curved arrows show the relative rolling motion of clusters, where red and green colors indicate constrained, and unconstrained motion, respectively. (f) Average total number of contacts per cluster (solid lines), and contacts per neighbor (dashed lines) for each cluster versus applied shear stress for two different area fractions exhibiting CST and DST behavior.

We also hypothesize that if two clusters are connected through a single particle-particle contact, their relative motion is constrained only with respect to the sliding friction. However, when two adjacent clusters are connected via multiple particle-level contacts, their rolling motion also becomes significantly hindered, since relative motion of clusters will require multiple two contacts to be made mobile. This is sketched in Figs. 4(d) and 4(e) for the two cases, to better illustrate the hindered motion of particle clusters. Thus, the total number of contacts [at the particle level] that each cluster makes with its surrounding clusters can bring an insight into their dynamics. The average number of total contacts between clusters, and their normalized values per cluster neighbor versus stress are plotted in Fig. 4(f). Deep into the STS, each cluster for the CST suspension is connected to its neighbors through a single force contact, i.e., constrained sliding motion. On the other hand, on average each DST cluster is connected with more than two contacts to a neighbor, i.e., sliding and rolling constraints. This suggests that although the nature of the contacts at the particle level is exactly the same for the two systems, one where particle clusters are overconstrained in their relative motion will exhibit DST whereas the single-mode hindrance to motion of clusters only results in CST behavior.

In summary, results presented here strongly suggest that a rigorous interrogation of the force networks in flowing suspensions can bring insight into their micro- and mesomechanics. Emergence of a percolated contact network of a highly heterogeneous nature is responsible for the onset of ST. These heterogeneities, however, diminish by increasing the applied stress and into the STS, through formation of alternative paths within the network, until virtually all particles within the suspension belong to a single network. We find that the characteristics of particle-level contacts, however, cannot help authoritatively distinguish the CST and DST. Thus, using a GMM algorithm we identified larger scale force clusters. These clusters in DST were found to be denser and more interconnected, suggesting that not only the individual load-bearing units are of more rigid nature in DST compared to CST, but also that denser connections between the clusters provide higher resistance to large deformations. Finally, a coarse-grained description of the contact network showed that multiple particle-level connections between neighboring force clusters in the DST regime effectively constrain the sliding and rolling motion of these mesoscale structures, while single connection between the CST clusters suggest only a sliding motion hindrance. This clearly indicated that although the microdynamics of the two systems are identical, the larger mesoscale structures formed as a result of these contacts can significantly differ, leading to drastic changes in macroscopic rheological measures of a complex system.

The research in the Jamali group at Northeastern University is partially supported by the National Science Foundation's Awards No. 2104869 and No. 2118962. A. S. acknowledges support from the Center for Hierarchical Materials Design (CHiMaD) under Award No. 70NANB19H005 (U.S. Dept. Commerce), and from the Army Research Office under Grants No. W911NF-19-1-0245, No. W911NF-20-2-0044, and No. W911NF-21-1-0038. The authors would also like to acknowledge fruitful discussions with J. Morris, L. Hsiao, and E. Del Gado.

*Corresponding author.
s.jamali@northeastern.edu
†Present address: Department of Macromolecular Science and Engineering, Case Western Reserve University, Cleveland, Ohio 44106, USA.

[1] J. Mewis and N. J. Wagner, *Colloidal Suspension Rheology* (Cambridge University Press, Cambridge, England, 2011).
[2] Norman J Wagner and John F Brady, Shear thickening in colloidal dispersions, Phys. Today **62**, No. 10, 27 (2009).
[3] Élisabeth Guazzelli and Jeffrey F. Morris, *A Physical Introduction to Suspension Dynamics* (Cambridge University Press, Cambridge, England, 2011).
[4] Morton M. Denn, Jeffrey F. Morris, and Daniel Bonn, Shear thickening in concentrated suspensions of smooth spheres in newtonian suspending fluids, Soft Matter **14**, 170 (2018).
[5] Jeffrey F. Morris, Shear thickening of concentrated suspensions: Recent developments and relation to other phenomena, Annu. Rev. Fluid Mech. **52**, 121 (2020).
[6] Abhinendra Singh, Sidhant Pednekar, Jaehun Chun, Morton M. Denn, and Jeffrey F. Morris, From Yielding to Shear Jamming in a Cohesive Frictional Suspension, Phys. Rev. Lett. **122**, 098004 (2019).
[7] Abhinendra Singh, Christopher Ness, Ryohei Seto, Juan J. de Pablo, and Heinrich M. Jaeger, Shear Thickening and Jamming of Dense Suspensions: The "Roll" of Friction, Phys. Rev. Lett. **124**, 248005 (2020).
[8] Shravan Pradeep, Mohammad Nabizadeh, Alan R. Jacob, Safa Jamali, and Lilian C. Hsiao, Jamming Distance Dictates Colloidal Shear Thickening, Phys. Rev. Lett. **127**, 158002 (2021).
[9] Safa Jamali and John F. Brady, Alternative Frictional Model for Discontinuous Shear Thickening of Dense Suspensions: Hydrodynamics, Phys. Rev. Lett. **123**, 138002 (2019).
[10] Mu Wang, Safa Jamali, and John F. Brady, A hydrodynamic model for discontinuous shear-thickening in dense suspensions, J. Rheol. **64**, 379 (2020).
[11] Chiao-Peng Hsu, Joydeb Mandal, Shivaprakash N. Ramakrishna, Nicholas D. Spencer, and Lucio Isa, Exploring the roles of roughness, friction and adhesion in discontinuous shear thickening by means of thermo-responsive particles, Nat. Commun. **12**, 1477 (2021).
[12] Bram Schroyen, Chiao-Peng Hsu, Lucio Isa, Peter Van Puyvelde, and Jan Vermant, Stress Contributions in Colloidal Suspensions: The Smooth, the Rough, and the Hairy, Phys. Rev. Lett. **122**, 218001 (2019).
[13] Chiao-Peng Hsu, Shivaprakash N. Ramakrishna, Michele Zanini, Nicholas D. Spencer, and Lucio Isa, Roughness-dependent tribology effects on discontinuous shear thickening, Proc. Natl. Acad. Sci. U.S.A. **115**, 5117 (2018).

[14] Lilian C. Hsiao, Safa Jamali, Emmanouil Glynos, Peter F. Green, Ronald G. Larson, and Michael J. Solomon, Rheological State Diagrams for Rough Colloids in Shear Flow, Phys. Rev. Lett. **119**, 158001 (2017).
[15] Abhinendra Singh, Grayson L. Jackson, Michael van der Naald, Juan J. de Pablo, and Heinrich M. Jaeger, Stress-activated constraints in dense suspension rheology, Phys. Rev. Fluids **7**, 054302 (2022).
[16] Ryohei Seto, Romain Mari, Jeffrey F. Morris, and Morton M. Denn, Discontinuous Shear Thickening of Frictional Hard-Sphere Suspensions, Phys. Rev. Lett. **111**, 218301 (2013).
[17] Romain Mari, Ryohei Seto, Jeffrey F. Morris, and Morton M. Denn, Shear thickening, frictionless and frictional rheologies in non-Brownian suspensions, J. Rheol. **58**, 1693 (2014).
[18] Matthieu Wyart and Michael E. Cates, Discontinuous Shear Thickening Without Inertia in Dense Non-Brownian Suspensions, Phys. Rev. Lett. **112**, 098302 (2014).
[19] Abhinendra Singh, Romain Mari, Morton M. Denn, and Jeffrey F. Morris, A constitutive model for simple shear of dense frictional suspensions, J. Rheol. **62**, 457 (2018).
[20] B. M. Guy, J. A. Richards, D. J. M. Hodgson, E. Blanco, and W. C. K. Poon, Constraint-Based Approach to Granular Dispersion Rheology, Phys. Rev. Lett. **121**, 128001 (2018).
[21] Safa Jamali, Emanuela Del Gado, and Jeffrey F. Morris, Rheology discussions: The physics of dense suspensions, J. Rheol. **64**, 1501 (2020).
[22] Jetin E. Thomas, Kabir Ramola, Abhinendra Singh, Romain Mari, Jeffrey F. Morris, and Bulbul Chakraborty, Microscopic Origin of Frictional Rheology in Dense Suspensions: Correlations in Force Space, Phys. Rev. Lett. **121**, 128002 (2018).
[23] Marcio Gameiro, Abhinendra Singh, Lou Kondic, Konstantin Mischaikow, and Jeffrey F. Morris, Interaction network analysis in shear thickening suspensions, Phys. Rev. Fluids **5**, 034307 (2020).
[24] Omer Sedes, Hernan A. Makse, Bulbul Chakraborty, and Jeffrey F. Morris, *K*-core analysis of shear-thickening suspensions, Phys. Rev. Fluids **7**, 024304 (2022).
[25] Steven H. Strogatz, Exploring complex networks, Nature (London) **410**, 268 (2001).
[26] Réka Albert and Albert-László Barabási, Statistical mechanics of complex networks, Rev. Mod. Phys. **74**, 47 (2002).
[27] Albert-László Barabási, Network science, Phil. Trans. R. Soc. A **371**, 20120375 (2013).
[28] Albert-László Barabási and Zoltán N. Oltvai, Network biology: Understanding the cell's functional organization, Nat. Rev. Genet. **5**, 101 (2004).
[29] Stephen Y. Chan and Joseph Loscalzo, The emerging paradigm of network medicine in the study of human disease, Circ. Res. **111**, 359 (2012).
[30] Ed Bullmore and Olaf Sporns, Complex brain networks: Graph theoretical analysis of structural and functional systems, Nat. Rev. Neurosci. **10**, 186 (2009).
[31] Lia Papadopoulos, James G. Puckett, Karen E. Daniels, and Danielle S. Bassett, Evolution of network architecture in a granular material under compression, Phys. Rev. E **94**, 032908 (2016).
[32] M. E. J. Newman, Modularity and community structure in networks, Proc. Natl. Acad. Sci. U.S.A. **103**, 8577 (2006).
[33] M. E. J. Newman and M. Girvan, Finding and evaluating community structure in networks, Phys. Rev. E **69**, 026113 (2004).
[34] Arman Boromand, Safa Jamali, Brandy Grove, and João M. Maia, A generalized frictional and hydrodynamic model of the dynamics and structure of dense colloidal suspensions, J. Rheol. **62**, 905 (2018).
[35] See Supplemental Material at http://link.aps.org/supplemental/10.1103/PhysRevLett.129.068001 for details on methods used, which includes Refs. [36–42].
[36] Joshua E. S. Socolar, David G. Schaeffer, and Philippe Claudin, Directed force chain networks and stress response in static granular materials, Eur. Phys. J. E **7**, 353 (2002).
[37] J. F. Peters, M. Muthuswamy, J. Wibowo, and A. Tordesillas, Characterization of force chains in granular material, Phys. Rev. E **72**, 041307 (2005).
[38] Trushant S. Majmudar and Robert P. Behringer, Contact force measurements and stress-induced anisotropy in granular materials, Nature (London) **435**, 1079 (2005).
[39] Mark Herrera, Shane McCarthy, Steven Slotterback, Emmanuel Cephas, Wolfgang Losert, and Michelle Girvan, Path to fracture in granular flows: Dynamics of contact networks, Phys. Rev. E **83**, 061303 (2011).
[40] Ulrik Brandes, Daniel Delling, Marco Gaertler, Robert Gorke, Martin Hoefer, Zoran Nikoloski, and Dorothea Wagner, On modularity clustering, IEEE transactions on knowledge and data engineering **20**, 172 (2007).
[41] P. A. Cundall and O. D. L. Strack, A discrete numerical model for granular assemblies, Geotechnique **29**, 47 (1979).
[42] Abhinendra Singh, Vanessa Magnanimo, Kuniyasu Saitoh, and Stefan Luding, The role of gravity or pressure and contact stiffness in granular rheology, New J. Phys. **17**, 043028 (2015).
[43] Neil Y. C. Lin, Christopher Ness, Michael E. Cates, Jin Sun, and Itai Cohen, Tunable shear thickening in suspensions, Proc. Natl. Acad. Sci. U.S.A. **113**, 10774 (2016).
[44] Safa Jamali, Arman Boromand, Norman Wagner, and Joao Maia, Microstructure and rheology of soft to rigid shear-thickening colloidal suspensions, J. Rheol. **59**, 1377 (2015).
[45] Romain Mari, Ryohei Seto, Jeffrey F. Morris, and Morton M. Denn, Discontinuous shear thickening in Brownian suspensions by dynamic simulation, Proc. Natl. Acad. Sci. U.S.A. **112**, 15326 (2015).
[46] Omer Sedes, Abhinendra Singh, and Jeffrey F. Morris, Fluctuations at the onset of discontinuous shear thickening in a suspension, J. Rheol. **64**, 309 (2020).
[47] John R. Royer, Daniel L. Blair, and Steven D. Hudson, Rheological Signature of Frictional Interactions in Shear Thickening Suspensions, Phys. Rev. Lett. **116**, 188301 (2016).
[48] Xiang Cheng, Jonathan H. McCoy, Jacob N. Israelachvili, and Itai Cohen, Imaging the microscopic structure of shear thinning and thickening colloidal suspensions, Science **333**, 1276 (2011).

[49] Kathryn A. Whitaker, Zsigmond Varga, Lilian C. Hsiao, Michael J. Solomon, James W. Swan, and Eric M. Furst, Colloidal gel elasticity arises from the packing of locally glassy clusters, Nat. Commun. **10**, 2237 (2019).

[50] Santo Fortunato and Darko Hric, Community detection in networks: A user guide, Phys. Rep. **659**, 1 (2016).

[51] Lia Papadopoulos, Mason A. Porter, Karen E. Daniels, and Danielle S. Bassett, Network analysis of particles and grains, J. Complex Netw. **6**, 485 (2018).